Lecture Notes in Electrical Engineering 405

Yingmin Jia
Junping Du
Weicun Zhang
Hongbo Li
Editors

Proceedings of 2016 Chinese Intelligent Systems Conference

Volume II

Springer

Lecture Notes in Electrical Engineering

Volume 405

Board of Series editors

Leopoldo Angrisani, Napoli, Italy
Marco Arteaga, Coyoacán, México
Samarjit Chakraborty, München, Germany
Jiming Chen, Hangzhou, P.R. China
Tan Kay Chen, Singapore, Singapore
Rüdiger Dillmann, Karlsruhe, Germany
Haibin Duan, Beijing, China
Gianluigi Ferrari, Parma, Italy
Manuel Ferre, Madrid, Spain
Sandra Hirche, München, Germany
Faryar Jabbari, Irvine, USA
Janusz Kacprzyk, Warsaw, Poland
Alaa Khamis, New Cairo City, Egypt
Torsten Kroeger, Stanford, USA
Tan Cher Ming, Singapore, Singapore
Wolfgang Minker, Ulm, Germany
Pradeep Misra, Dayton, USA
Sebastian Möller, Berlin, Germany
Subhas Mukhopadyay, Palmerston, New Zealand
Cun-Zheng Ning, Tempe, USA
Toyoaki Nishida, Sakyo-ku, Japan
Bijaya Ketan Panigrahi, New Delhi, India
Federica Pascucci, Roma, Italy
Tariq Samad, Minneapolis, USA
Gan Woon Seng, Nanyang Avenue, Singapore
Germano Veiga, Porto, Portugal
Haitao Wu, Beijing, China
Junjie James Zhang, Charlotte, USA

About this Series

"Lecture Notes in Electrical Engineering (LNEE)" is a book series which reports the latest research and developments in Electrical Engineering, namely:

- Communication, Networks, and Information Theory
- Computer Engineering
- Signal, Image, Speech and Information Processing
- Circuits and Systems
- Bioengineering

LNEE publishes authored monographs and contributed volumes which present cutting edge research information as well as new perspectives on classical fields, while maintaining Springer's high standards of academic excellence. Also considered for publication are lecture materials, proceedings, and other related materials of exceptionally high quality and interest. The subject matter should be original and timely, reporting the latest research and developments in all areas of electrical engineering.

The audience for the books in LNEE consists of advanced level students, researchers, and industry professionals working at the forefront of their fields. Much like Springer's other Lecture Notes series, LNEE will be distributed through Springer's print and electronic publishing channels.

More information about this series at http://www.springer.com/series/7818

Yingmin Jia · Junping Du
Weicun Zhang · Hongbo Li
Editors

Proceedings of 2016 Chinese Intelligent Systems Conference

Volume II

Springer

Editors
Yingmin Jia
Beihang University
Beijing
China

Junping Du
Beijing University of Posts
and Telecommunications
Beijing
China

Weicun Zhang
University of Science and Technology
Beijing
Beijing
China

Hongbo Li
Tsinghua University
Beijing
China

ISSN 1876-1100 ISSN 1876-1119 (electronic)
Lecture Notes in Electrical Engineering
ISBN 978-981-10-2334-7 ISBN 978-981-10-2335-4 (eBook)
DOI 10.1007/978-981-10-2335-4

Library of Congress Control Number: 2016948594

© Springer Science+Business Media Singapore 2016
This work is subject to copyright. All rights are reserved by the Publisher, whether the whole or part of the material is concerned, specifically the rights of translation, reprinting, reuse of illustrations, recitation, broadcasting, reproduction on microfilms or in any other physical way, and transmission or information storage and retrieval, electronic adaptation, computer software, or by similar or dissimilar methodology now known or hereafter developed.
The use of general descriptive names, registered names, trademarks, service marks, etc. in this publication does not imply, even in the absence of a specific statement, that such names are exempt from the relevant protective laws and regulations and therefore free for general use.
The publisher, the authors and the editors are safe to assume that the advice and information in this book are believed to be true and accurate at the date of publication. Neither the publisher nor the authors or the editors give a warranty, express or implied, with respect to the material contained herein or for any errors or omissions that may have been made.

Printed on acid-free paper

This Springer imprint is published by Springer Nature
The registered company is Springer Nature Singapore Pte Ltd.
The registered company address is: 152 Beach Road, #22-06/08 Gateway East, Singapore 189721, Singapore

Contents

Autonomous Control of Mobile Robots for Opening Doors Based on Multi-sensor Fusion

Xiaomei Ma and Chaoli Wang

Abstract This paper presents a method of opening doors by mobile robots autonomously. Considering that the existing fingerprint lock will collapse when finger injures, the use of robot shows its durability and convenience, and it avoids carrying even losing keys trouble, and incarnates people's awareness of intelligent robot era. In this robot opening door system, a mobile phone is applied to send open-door command, the robot receives the command via Wi-Fi, then plans path based on laser sensor and encoder sensors to move to the door position, and aims at the door handle based on visual servo, and finally opens the door. Experiments have proved the validity and feasibility of the presented method. Meanwhile, we are discussing other applications of this method.

Keywords Service robot · Path planning · Multi-sensor fusion · Inverse kinematics

1 Introduction

Nowadays, the application of mobile robots is expanding extremely, not only in industry, agriculture, national defense, service industry, but also in mine, hunting, rescue, radiation, and space field such as harmful and dangerous occasions, and all these fields receive very good application [1]. Being an active research area for a long time, autonomous robotics has attracted more and more attention [2]. Taking sweeping robot for example, it comes into millions of households and is accepted by more and more ordinary people.

X. Ma (✉) · C. Wang
Control Science and Engineering, University of Shanghai for Science and Technology, Shanghai 200093, China
e-mail: april_2016@163.com

C. Wang
e-mail: clclwang@126.com

© Springer Science+Business Media Singapore 2016

Y. Jia et al. (eds.), *Proceedings of 2016 Chinese Intelligent Systems Conference*, Lecture Notes in Electrical Engineering 405,
DOI 10.1007/978-981-10-2335-4_1

Navigation technology is one of the core technologies of mobile robots. The main navigation methods include: magnetic navigation, inertial navigation, GPS navigation, road navigation, visual navigation, voice navigation, and so on. GPS navigation systems can be found in motor vehicles and other various land-based vehicles. Paper [3] concludes that the accuracy of the GPS position fixes has a significant impact on the relative contributions that each dead-reckoning navigation sensor error makes. The RGB-D (Kinect-style) camera provides high quality synchronized videos of both color and depth, and dramatically increases robotic object recognition, manipulation, navigation, and interaction capabilities [4, 5]. Paper [6] presents an incremental method for concurrent mapping and localization for mobile robots equipped with 2D laser range finders, and illustrates that accurate maps of large, cyclic environments can be generated even in the absence of any odometric data. This paper adopts laser positioning and navigation to resolve path planning problem in the environment with complex obstacles.

This paper focuses on the navigation based on the laser scanner and encoder sensors, the positioning of the door handle based on Kinect, and the inverse kinematics of the manipulator.

2 System Description

This system is designed for mobile robots to open doors autonomously as long as users send open command. Figure 1 is a flowchart showing an overall operation of the system.

The difficulties mainly lie in the path planning and navigation of mobile robot in the environment with complex obstacles, the alignment of the door handle with robot, and the inverse kinematics of the manipulator.

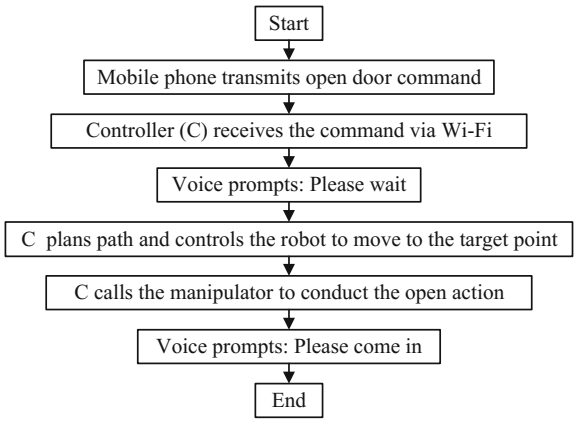

Fig. 1 The overall operation of the system

3 Laser Positioning and Navigation

The indoor map information is stored in the configuration file in advance, If in a new environment, the configuration file needs to be modified.

In order to achieve navigation and path planning of mobile robot in the environment with complex obstacles, this paper combines laser scanner with encoder sensors to achieve the best positioning effect. Laser scanner data and the robot current pose are used to update the map.

A-star algorithm is used to plan the path [7–9]. The planned path, which are a series of inflection points are recorded. The speed and the motion direction of the robot is calculated according to the robot's current pose and the target (door) position, the robot is controlled to move along the inflection points until it arrives at the target point. The navigation and path planning program interface is shown in Fig. 2.

Left is map display part, which is responsible for the real-time display of the map and path. Right top is the laser scanner device connection part. Right center is motion control part, which is designed to control the robot to move forward, backward, turn left, turn right, and stop. Right bottom is target point input part. Robot pose part is used to set the robot current pose.

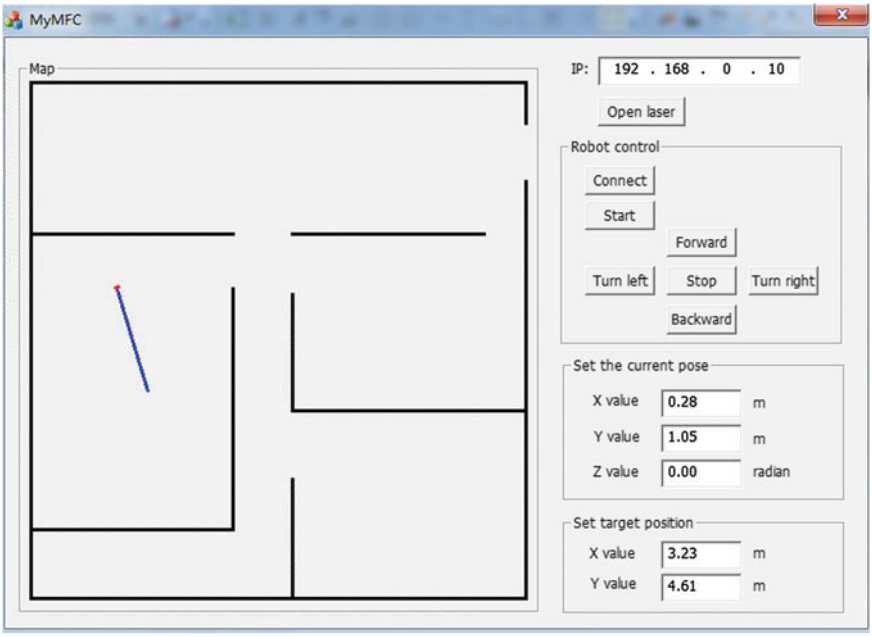

Fig. 2 The navigation and path planning program interface

4 Control Algorithm of the Manipulator

The open action is realized by manipulator rotating the door handle. Manipulator aligns door handle is the premise. However, manipulator usually misaligns the door handle when robot arrives at the door position.

This paper adopts a Kinect to obtain the target position. Since Kinect is RGB-D style, it provides both color and depth information. A red square mark is used to solve the alignment problem. The centroid of the red square is installed at the same vertical line with the door handle. The alignment is achieved by aligning the manipulator with the red marker. By handling the video captured by Kinect, robot is controlled to move right or left to align the red mark. Figure 3 shows the red mark and its extraction. Mathematical morphology is applied in the process of digital image processing [10–12].

The deployed manipulator is four DOF. D-H method is used to establish the coordinate frames [13]. The manipulator with D-H link coordinate frames is shown in Fig. 4.

Table 1 displays the D-H link parameter. Coordinate frame $i-1$ can be transformed into i through the following consecutive relative movement:

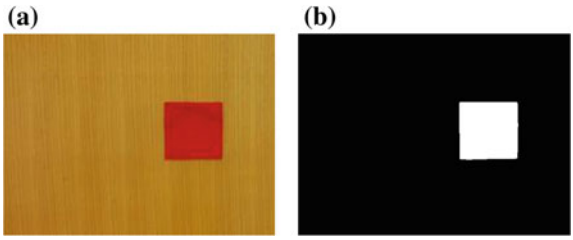

Fig. 3 The red mark and its extraction

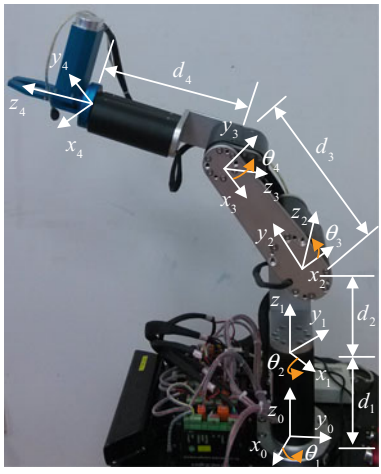

Fig. 4 The manipulator with D-H link coordinate frames

Table 1 D-H parameter

i	a_i	α_i	d_i	θ_i
1	0	0	d_1 (constant)	θ_1
2	0	$\pi/2$	d_2 (constant)	θ_2
3	0	0	d_3 (constant)	θ_3
4	0	$\pi/2$	d_4 (constant)	θ_4

Step 1 Translate d_i from x_{i-1} to x_i along z_{i-1}.
Step 2 Rotate θ_i angle from x_{i-1} to x_i about z_{i-1}, $\theta_i \in (-\pi, \pi]$.
Step 3 Translate a_i from z_{i-1} to z_i along x_i.
Step 4 Rotate angle α_i from z_{i-1} to z_i about x_i. $\alpha_i \in (-\pi, \pi]$.

The homogeneous transformation matrix of the continuous relative transformation is defined as

$$A_i^{i-1} = \mathrm{Trans}_z(d_i)\mathrm{Rot}_z(\theta_i)\mathrm{Trans}_x(a_i)\mathrm{Rot}_x(\alpha_i) = \begin{bmatrix} c_i & -c\alpha_i s_i & s\alpha_i s_i & a_i c_i \\ s_i & c\alpha_i c_i & -s\alpha_i c_i & a_i s_i \\ 0 & s\alpha_i & c\alpha_i & d_i \\ 0 & 0 & 0 & 1 \end{bmatrix} \tag{1}$$

where $s_i \triangleq \sin\theta_i, c_i \triangleq \cos\theta_i, s\alpha_i \triangleq \sin\alpha_i, c\alpha_i \triangleq \cos\alpha_i$.

Substituting D-H parameter in Table 1 into Eq. (1) leads to

$$A_4^0 = A_1^0 A_2^1 A_3^2 A_4^3 = \begin{bmatrix} c_{12}c_{34} & s_{12} & c_{12}s_{34} & d_3 s_{12} + d_4 s_{12} \\ s_{12}c_{34} & -c_{12} & s_{12}s_{34} & -d_3 c_{12} - d_4 c_{12} \\ s_{34} & 0 & -c_{34} & d_1 + d_2 \\ 0 & 0 & 0 & 1 \end{bmatrix} \tag{2}$$

where $c_{ij} \triangleq \cos(\theta_i + \theta_j), s_{ij} \triangleq \sin(\theta_i + \theta_j)$.

It needs to control the gripper of the manipulator to move to the door handle position. The pose of gripper can be obtained as long as the robot aligns the door handle with the known height of door handle and the distance between it and robot which is obtained from the Kinect. Namely, A_4^0 is known, each joint variable $q = [q_1, q_2, q_3, q_4]^T$ should be solved according to the joint conversion relationship, which belongs to classic inverse kinematics of robot [13].

The joints 2 and 3 of the manipulator are mainly controlled. The simplified model is shown in Fig. 5. The angle coordinates of the two joints (q_1, q_2) are solved from the coordinates of the end of the manipulator (z_1, y_1) in working space.

Doing geometric analysis according to Fig. 5 leads to Eq. (3)

$$\begin{cases} z_1 = l_1 \sin(q_1) + l_2 \sin(q_1 + q_2) \\ y_1 = l_1 \cos(q_1) + l_2 \cos(q_1 + q_2) \end{cases} \tag{3}$$

Solving Eq. (3) leads to Eqs. (4) and (5)

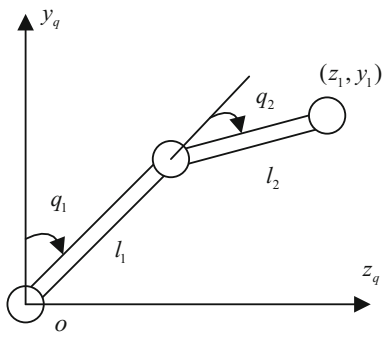

Fig. 5 The simplified two-DOF structure

$$q_1 = \arccos\left(\frac{z_1^2 + y_1^2 - l_1^2 - l_2^2}{2l_1 l_2}\right) \tag{4}$$

$$q_2 = \begin{cases} p_1 - p_2, q_1 > 0 \\ p_1 + p_2, q_1 \leq 0 \end{cases} \tag{5}$$

where $p_1 = \arctan\frac{y_1}{z_1}, p_2 = \arccos\left(\frac{z_1^2 + y_1^2 - l_1^2 - l_2^2}{2l_1\sqrt{z_1^2 + y_1^2}}\right)$.

5 Experiment Results

In order to verify the effectiveness of the proposed method, a mobile robot equipped with two 70 W DC motors and optical encoders with a precision level of 500 pulses rotation were used.

As shown in Fig. 6, the mobile robot is equipped with a laser scanner, a Kinect, a four-DOF manipulator with a single-DOF gripper. The UST-10LX model laser scanner communicates with the interface via internet. The 2D plane measuring range of the laser scanner is 270° with angular resolution of 0.25°. The maximum measuring distance is 30 m. The main controller was designed with a PC. The robot can be controlled by two motors to move forward, backward, left, right, and stop. Figure 6 shows the movie snapshot of the process of opening the door.

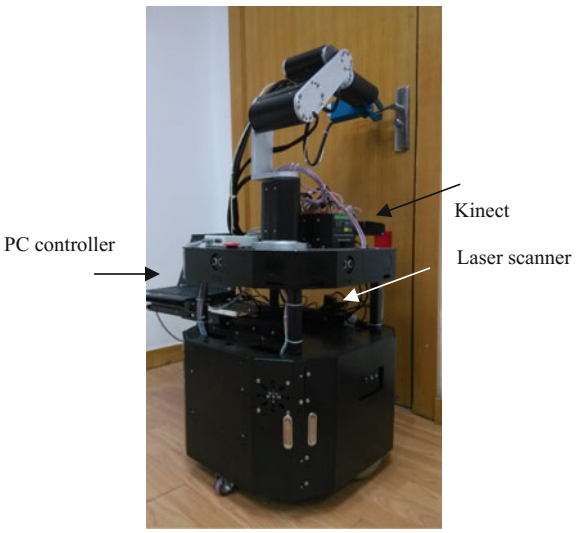

Fig. 6 The mobile robot for experiment

6 Conclusion

This paper presents a method of opening doors by mobile robots autonomously. In the robot opening door system, all users need to do is to apply a mobile phone to send the open command. The robot receives the command via Wi-Fi, then plans path to move to the door position based on laser scanner and encoder sensors, and aims at the door handle based on visual servo, finally opens the door autonomously. The use of robot shows its advantage over other methods. It is not only durable but also convenient. Besides, sometimes we come back home without keys, this method avoids carrying even losing keys trouble. In addition, with more and more autonomous robots coming into millions of households, the use of robot incarnates people's awareness of intelligent robot era and pursuit of science and fashion. Experiments have proved the validity and feasibility of the presented method. Meanwhile, we are discussing other applications of this method.

References

1. Xu BG, Yin YX, Zhou MJ (2007) Present situation and Prospect of intelligent mobile robot [J]. Robot Technol Appl 2:29–34
2. Sakagami Y, Watanabe R, Aoyama C, et al. (2002) The intelligent ASIMO: system overview and integration. IEEE/RSJ Int Conf Intell Robots Syst 3:2478–2483
3. Abbott E, Powell D (1999) Land-vehicle navigation using GPS. Proc IEEE 87(1):145–162
4. Lai K, Bo L, Ren X, et al. (2011) A large-scale hierarchical multi-view RGB-D object dataset. In: IEEE International conference on robotics and automation, pp 1817–1824

5. Sturm J, Engelhard N, Endres F, et al. (2012) A benchmark for the evaluation of RGB-D SLAM systems. In: 2012 IEEE/RSJ international conference on intelligent robots and systems, pp 573–580
6. Thrun S, Burgard W, Fox D (2000) A real-time algorithm for mobile robot mapping with applications to multi-robot and 3D mapping. In: IEEE international conference on robotics and automation, vol 1, pp 321–328
7. Cheng LP, Liu CX, Yan B (2014) Improved hierarchical A-star algorithm for optimal parking path planning of the large parking lot. In: 2014 IEEE international conference on information and automation, pp 695–698
8. Zhang Y, Tang GJ, Chen L (2012) Improved A-star algorithm for time dependent vehicle routing problem. Control Eng China 19(5):750–756
9. Yao J, Lin C, Xie X, et al. (2010) Path planning for virtual human motion using improved A* star algorithm. IN: 2010 seventh international conference on information technology: new generations, pp 1154–1158
10. Cui Y (2002) Image processing and analysis: the method and application of mathematical morphology [M]. Science Press, Beijing
11. Li JS, Li XH (2007) Digital image processing [M]. Tsinghua University Press, Beijing, pp 225–248
12. Zhu XC, Liu F, Hu D (2014) Digital image processing and image communication [M]. Beijing university of posts and telecommunications press, Beijing
13. Huo W (2005) Robots dynamics and control [M]. Higher Education Press, Beijing

Linear Active Disturbance Rejection Control Approach for Load Frequency Control Problem Using Diminishing Step Fruit Fly Algorithm

Congzhi Huang and Yan Li

Abstract The diminishing step fruit fly optimization algorithm (DS-FOA) is employed to optimize the performance of the load frequency control (LFC) problem by employing the linear active disturbance rejection control (LADRC) approach. First of all, the LFC problem taking into account the case of a single generator supplying power to a single service area is presented. Second, the general LADRC solution to the problem is given, where the diminishing step fruit fly optimization algorithm (DS-FOA) is employed to optimize the performance of the system with the approach. Third, the performances of the system with the following three control approaches are compared, including the traditional PID control approach, the normal LADRC approach, and the DS-FOA optimized LADRC approach. With the proposed LADRC approach, the system performance is much better than that of the traditional PID controller, and a much better performance is achieved with the proposed DS-FOA optimized LADRC approach. The performance superiority of the proposed approach is also validated by the frequency domain analysis results given.

Keywords Fruit fly optimization algorithm (FOA) · Load frequency control (LFC) · Linear active disturbance rejection control (LADRC) · Power system

1 Introduction

The problem to control the active power output of generating units responding to the disturbances in grid frequency and tie line power exchange within the designated limitation is denoted by the load frequency control issue [1]. Nowadays, it has

C. Huang (✉) · Y. Li
School of Control and Computer Engineering, North China Electric Power University, Beijing 102206, China
e-mail: hcz190@ncepu.edu.cn

Y. Li
e-mail: liyan_kj@ncepu.edu.cn

© Springer Science+Business Media Singapore 2016

Y. Jia et al. (eds.), *Proceedings of 2016 Chinese Intelligent Systems Conference*, Lecture Notes in Electrical Engineering 405,
DOI 10.1007/978-981-10-2335-4_2

become a hot topic with the aggressive development of smart grid all over the world. The traditional PID control strategy is usually employed to solve the LFC problem. The particle swarm optimized PID control approach is proposed in [2], and the other approaches refer to the model predictive control [3], adaptive fuzzy logic control [4], robust $H\infty$ control [5], and so on.

However, the performance improvement of the system with the traditional PID control approach is usually limited, while most of the advanced control approaches are difficult to put into practice due to its complex structure. To solve the disturbance rejection control problem widespread in industry, the active disturbance rejection control approach by Han [6] was brought into being. Its core idea is that the total disturbance, including all the internal uncertainties and external disturbance can be estimated with the aid of an extended state observer constructed in real time, and then cancelled by the nonlinear PD control law [7]. However, there were too many parameters to be tuned in the original ADRC approach, and thus it is often difficult to conduct parameter tuning work and put it into practice. Fortunately, the linear version of the ADRC approach emerges at a historic moment in [8], which largely simplified the parameters tuning procedure and thus quickly found a number of applications in practical engineering, see the integrated guidance and control system [9], and the hot strip width and gauge regulation problem [10].

In this paper, a general LADRC approach is introduced, and the DS-FOA is employed to tune the LADRC approach. In addition, the LFC problem for the single area power system with a non-reheated turbine is given for an example. A fourth-order LADRC approach is used to illustrate the effectiveness of the proposed approach. In order to improve the system performance, the DS-FOA is employed to tune the parameters in the LADRC approach, the result is also compared with that of the traditional PID approach in [11] and the normal LADRC approach in [12].

2 LFC Problem Formulation

A linear model of a single area power system with a non-reheated turbine is shown in Fig. 1.

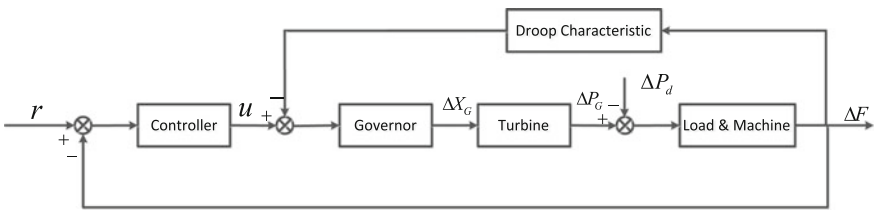

Fig. 1 Linear model of a single area power system

As can be seen from Fig. 1, r is the reference input, u is the controller output, and ΔF is the frequency deviation, which is also the controlled process output in the load frequency control problem. ΔP_d represents the external load disturbance, ΔP_G represents the incremental quantity in generator output, and ΔX_G the incremental quantity in governor valve position.

The plant discussed in this paper is the same with that in [11] consisting of the following three parts: governor, turbine, and load and machine. The dynamics of the governor can be described as $G_g(s) = 1/(T_g s + 1)$, and the turbine model is often represented by $G_t(s) = 1/(T_t s + 1)$. The transfer function of the load and machine is denoted by $G_m(s) = K_p/(T_p s + 1)$. In addition, the droop characteristic is a feedback controller with the gain of $1/R$ so as to improve the system performance.

Since the LFC problem for the power system under consideration is expressed only to relatively small changes in load, so the controller can be used to ensure the frequency deviation as small as possible under small load changes.

3 Linear Active Disturbance Rejection Control Solution

A. *Linear Active Disturbance Rejection Control*

The typical block diagram for the system with the LADRC approach is shown in Fig. 2.

As shown in Fig. 2, an ESO based on the process input and output data is constructed to estimate the process output its finite time derivatives, and the total disturbance. Consider the following general controlled process:

$$y^{(n)} = g(t, y, \dot{y}, \ldots, u, \dot{u}, \ldots, w) + bu, \tag{1}$$

where y is the controlled process output variable, u is the control input, and w represents the external disturbance. Taking the estimation value of b as b_0, it can be rewritten as:

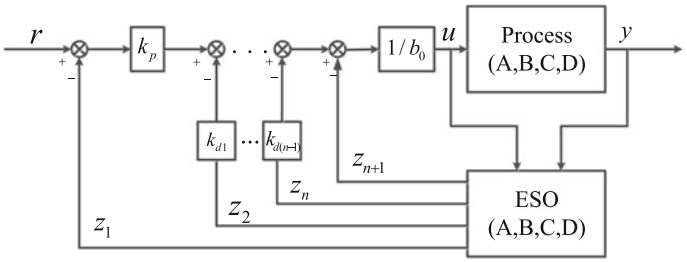

Fig. 2 Block diagram of control system with the LADRC approach

$$y^{(n)} = g(t, y, \dot{y}, \ldots, u, \dot{u}, \ldots, w) + (b - b_0)u + b_0 u = f + b_0 u, \tag{2}$$

where $f = g(t, y, \dot{y}, \ldots, u, \dot{u}, \ldots, w) + (b - b_0)u$ is defined as the total disturbance, including the unknown dynamics as well as all the external disturbances. Define an augmented state vector $x = [x_1, x_2, \ldots, x_n, x_{n+1}]^T$, the extended state equation of the original process is given as follows:

$$\begin{cases} \dot{x}_1 = x_2 \\ \ldots \\ \dot{x}_n = x_{n+1} + b_0 u \\ \dot{x}_{n+1} = h \\ y = x_1 \end{cases}, \tag{3}$$

where the state variables $x_1, x_2, \ldots, x_n$ are the process state, $x_{n+1} = f$ added as an augmented state, and $h = f'$ is the unknown variable representing the first order time derivative of the total disturbance.

Then, the following extended state observer is constructed:

$$\begin{cases} \dot{z}_1 = z_2 + \beta_1 (y(t) - z_1) \\ \ldots \\ \dot{z}_n = z_{n+1} + \beta_n (y(t) - z_1) + b_0 u \\ z_{n+1} = \beta_{n+1} (y(t) - z_1) \end{cases}, \tag{4}$$

where the observer gain is denoted by $L = [\beta_1, \beta_2, \ldots, \beta_n, \beta_{n+1}]^T$. With appropriate observer gains, the following state variables can be tracked accurately:

$$\begin{aligned} &z_1(t) \to y(t), z_2(t) \to \dot{y}(t), \ldots, z_n(t) \to y^{(n-1)}(t) \\ &z_{n+1}(t) \to f \end{aligned} \tag{5}$$

In order to simplify the parameter tuning procedure of the ESO, all the observer poles are placed at the same place $-\omega o$, where the observer bandwidth w_o is the only parameter to be tuned. The characteristic equation of the ESO is given as:

$$s^n + \beta_1 s^{n-1} + \cdots + \beta_{n-1} s + \beta_n = (s + \omega_o)^n. \tag{6}$$

Then, the ESO gain L can be obtained as follows: $\beta_1 = n\omega_o$, $\beta_2 = 0.5n(n-1)\omega_o^2, \ldots, \beta_o = n\omega_o^n$, $\beta_{n+1} = \omega_o^{n+1}$. With the well-tuned ESO, the control law is then designed:

$$u = \frac{-z_{n+1} + u_0}{b_0} \tag{7}$$

This control law reduces the original plant to a cascaded integrator, which can be easily controlled by a PD controller as follows:

$$u_0 = k_p(r - z_1) - k_{d1}z_2 - \cdots - k_{d(n-1)}z_n \tag{8}$$

After the gains are selected in order to place all the roots of the closed-loop characteristic equation at the same place $-\omega_c$, where w_c is the controller bandwidth.

$$s^n + k_{d(n-1)}s^{n-1} + \cdots + k_{d1}s + k_p = (s + \omega_c)^n, \tag{9}$$

where the controller parameters k_p, k_{d1},…, $k_{d(n-1)}$ are chosen as follows: $k_p = \omega_c^n$, $k_{d1} = \omega_c^{n-1}$,…, $k_{d(n-1)} = n\omega_c$.

Now, there are only three parameters to be tuned in the LADRC approach: b_0, ω_c and ω_o. In the following section, the FOA will be employed to tune them so as to achieve better performance.

B. *Fruit Fly Optimization Algorithm*

The fruit fly optimization algorithm (FOA) proposed by Pan [13] is a kind of swarm intelligent algorithm. Compared with the traditional particle swarm optimization (PSO) algorithm, the FOA can achieve an optimal speed. But it also has its own disadvantages: it is easy to fall into a local optimal solution, and it is easy to become premature. Thus there are many scholars trying to improve the traditional FOA. The diminishing step fruit fly optimization algorithm (DS-FOA) is proposed in [14] to improve the global searching ability at the beginning and ensure the local optimization ability later. In the DS-FOA, the searching step length L changes from a constant variable into a decline variable:

$$L = L_0 - \frac{L_0(G-1)}{G_{\max}}, \tag{10}$$

where L_0 is the initial searching step length, G is the current optimization iteration number and $G_{\max}$ *is* the max optimization iteration number. The tuning procedure of the DS-FOA optimized LADRC approach is given as follows:

Step 1 Initialization. Set the max optimization iteration number $G_{\max}$, and the flies population size P.

Step 2 Generate the initial locations of the fruit fly swarm randomly, $\theta_0 = [(x_{01}, y_{01}), (x_{02}, y_{02}), (x_{03}, y_{03})]$.

Step 3 Use (10)–(12) to assign each fruit fly a direction and distance randomly, and change the searching step L.

$$X(i) = X_{0i} + L * \text{rand}(1,1) \tag{11}$$

$$Y(i) = Y_{0i} + L * \text{rand}(1,1) \tag{12}$$

Step 4 Take the values of the parameters b_0, ω_c and ω_o into the LADRC approach, and obtain the system error $e(t) = y(t) - r(t)$, where y is the system output,

and r is the set point. The performance index ITAE (Integration of Time multiplied by Absolute Error) can be selected as the fitness function.

$$J = \int_0^\infty t|e(t)|\mathrm{d}t \tag{13}$$

Based on Eq. (13), the value of performance index J can be easily obtained.

Step 5 Compute the minimum value of $J_{\min}$ and the location of b_0, ω_c and ωo: $\theta_i = [(x_{i1}, y_{i1}), (x_{i2}, y_{i2}), (x_{i3}, y_{i3})]$

Step 6 Once $J_{\min,}$ is obtained, update the initial location as $\theta_0 = [(x_{ib0}, y_{ib0}), (x_{i\omega c}, y_{i\omega c}), (x_{i\omega o}, y_{i\omega o})]$.

Step 7 Repeat step 3–6. When it comes to achieve maximum iteration number then run out of circulation, and get the final values of b_0, ω_c and ω_o.

4 Illustrative Examples

The nominal parameters of the non-reheated turbine plant in Fig. 1 are chosen as follows: $K_p = 120$, $T_p = 20$, $T_t = 0.3$, $T_g = 0.08$, and $R = 2.4$. With the given nominal parameters, the process model with droop characteristic can be obtained as $G_p(s) = 250/(s^3 + 15.88s^2 + 42.46s + 106.2)$. To verify the robustness of the proposed approach, the parameters of the system are assumed to vary by ±50 %. $1/T_t \in [2.564, 4.762]$, $1/T_g \in [9.615, 17.857]$, $1/T_p \in [0.033, 0.1]$, $K_p/T_p \in [4, 12]$, $1/RT_g \in [3.081, 10.639]$.

The PID controller $K(s) = 0.4036 + 0.6356/s + 0.1832s$ was the one adopted in [11]. The LADRC tuning parameters in [12] are selected as follows: the estimation value $b = 250$, the observer bandwidth $\omega_o = 5.15$ and the controller bandwidth $\omega_c = 280$.

In the DS-FOA optimized LADRC approach, the population size is set as 30, the number of iterations is chosen as 20, and the initial searching step length is equal to 1, and the simulation results are presented in Fig. 3. Figure 4 shows the optimization processes of DS-FOA. Table 1 shows the optimization result.

A. *Disturbance Rejection Test*

After conducting a disturbance rejection test, the performance superiority of the optimized LADRC approach can be verified. With the load demand $\Delta P_d = 0.01$, the responses of the power system with non-reheated turbine and the DS-FOA optimized LADRC approach are shown and compared with the PID and LADRC performance from [11, 12] in Fig. 4.

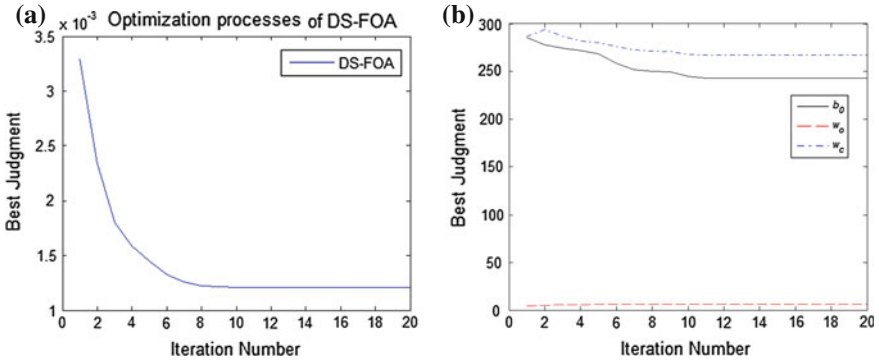

ITAE Optimization processes; LADRC parameters optimization processes

Fig. 3 Optimization processes of DS-FOA

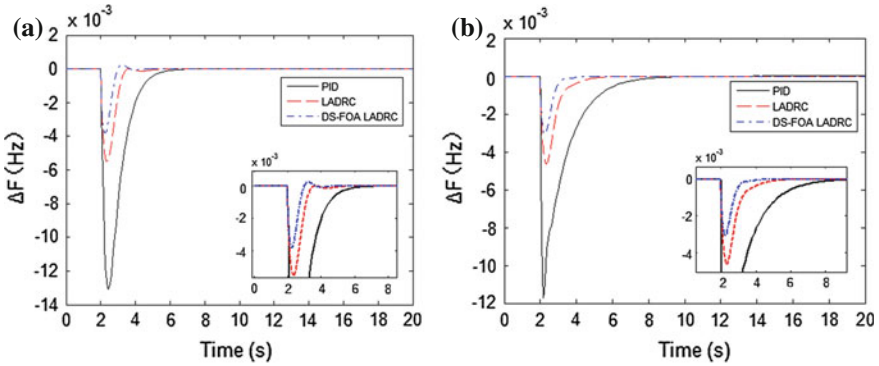

Nominal parameters; Upper bound;

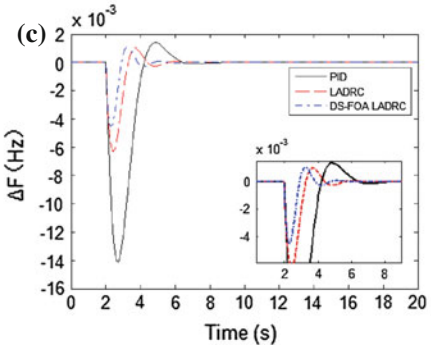

Lower bound

Fig. 4 The responses of power system with a non-reheated turbine and the following three control approaches: PID, LADRC and DS-FOA optimized LADRC approach

Table 1 Result of DS-FOA optimization LADRC parameters

b_0	ω_c	ω_o	ITAE
242.6164	267.1187	6.3466	0.001208

As shown in Fig. 4, the performance of the system with the fourth-order LADRC is much better than that of PID controller. In addition, by using DS-FOA optimize LADRC parameters, the system shows a much better performance.

B. *Performances Indices*

To further compare the performance of the system with the DS-FOA optimized LADRC approach with that of the PID controller and the normal LADRC approach, the performance indices ITAE are computed and listed in Table 2.

In this table, it is shown that with the DS-FOA optimized LADRC approach in the system, the performance indices are much smaller than the other two control approaches, which explicitly indicates that the performance superiority of the proposed approach.

C. *Open Loop Transfer Function Frequency Domain Analysis*

For the unit negative feedback control system, the actuator is assumed to be linear and its gain is equal to 1. Its open loop transfer function is $G_{cloop}(s) = G_p * G_c$, where G_p is plant transfer function and G_c is controller transfer function. It is easy to know the transfer function of plant G_p and the PID controller G_{cPID} from [11].

$$G_{cPID}(s) = 0.4036 + \frac{0.6356}{s} + 0.1832s \tag{14}$$

In [15], the transfer function of LADRC has been summarized. For this paper, the transfer function of LADRC and DS-FOA LADRC can be expressed as follows:

$$G_{\mathrm{CLADRC}}(s) = \frac{2.195\times10^7 s^4 + 4.522\times10^8 s^3 + 3.493\times10^9 s^2 + 1.199\times10^{10} s + 1.544\times10^{10}}{250s^3 + 2.195\times10^7 s^2 + 2.68\times10^7 s + 2.693\times10^7} \tag{15}$$

$$G_{\mathrm{CDLADRC}}(s) = \frac{1.849\times10^7 s^4 + 4.602\times10^8 s^3 + 4.296\times10^9 s^2 + 1.782\times10^{10} s + 2.773\times10^{10}}{240s^3 + 1.849\times10^7 s^2 + 2.371\times10^7 s + 2.389\times10^7} \tag{16}$$

Table 2 The Performance Indices ITAE

Controller	Optimized LADRC	LADRC	PID
ITAE	0.00121/0.00110/0.00197	0.0069/0.0077/0.0104	0.0302/0.0365/0.0329

Note ITAE performance indices are presented in order as the system with the normal/upper bound/lower bound parameters

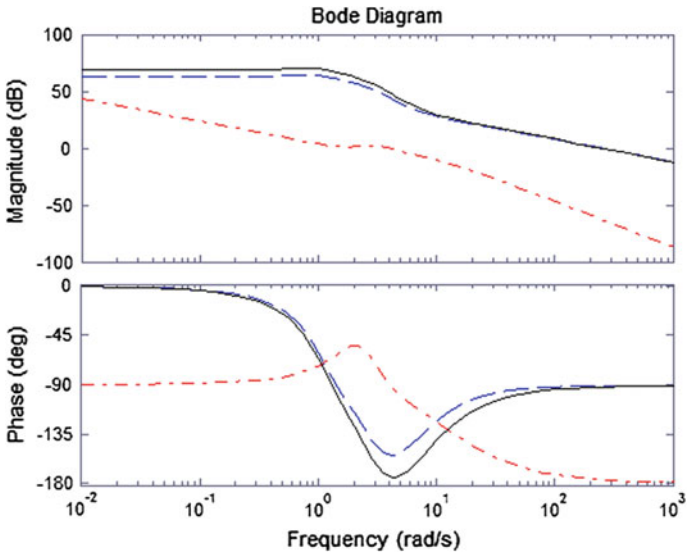

Fig. 5 Frequency domain analysis of PID controller, LADRC and DS-FOA optimized LADRC (*solid* LADRC; *dashed* DS-FOA optimized LADRC; *dash dotted* PID)

Table 3 Open loop transfer function frequency domain analysis

Controller	PM dB (Cut-off frequency rad/sec)
PID	92.3273 (3.8749)
LADRC	89.0296 (249.8372)
DS-FOA LADRC	88.0407 (249.9800)

The Bode plots for the open loop transfer functions of the system with the three controllers are shown in Fig. 5.

As can be seen from Fig. 5 and Table 3, all the three controllers make the system stable. The LADRC increase the cut-off frequency to achieve a better response speed than the traditional PID control approach. By using the DS-FOA optimized LADRC parameters, the system has a higher phase margin in middle frequency so that it has a better dynamic characteristics, which also proves the performance superiority of the proposed approach.

5 Conclusion

In this paper, the DS-FOA optimized LADRC approach is proposed, and its performance superiority is validated by the simulation example. By using DS-FOA tuning the three control parameters of LADRC, b_0, ω_o and ω_c, the LFC problem in this paper is solved. The performance of LADRC demonstrates the effectiveness

and robustness of the proposed LADRC approach. In addition, by using the DS-FOA, the better parameters of LADRC can be found and the controller achieved better effect and stronger robustness. However, its deficiency is that the performance of the FOA can be improved further, and the optimized parameters of LADRC by DS-FOA for the reheated turbine plant and hydroturbine plant remains a difficult and challenging problem to be further investigated.

Acknowledgments This work is supported by National Natural Science Foundation of China under Grant 61304041, and the Fundamental Research Funds for the Central Universities 2016ZZD03.

References

1. Kundur P (1994) Power system stability and control. McGraw-Hill, New York
2. Kouba NEY, Menaa M, Hasni M, et al. (2014) Optimal load frequency control in interconnected power system using PID controller based on particle swarm optimization. In: International conference on electrical sciences and technologies in Maghreb, pp 1–8
3. Shi X, Hu J, Yu J, et al. (2015) A novel load frequency control strategy based on model predictive control. In: IEEE power and energy society general meeting, pp 1–5
4. Yousef H, Al-Kharusi K, Albadi MH et al (2014) Load frequency control of a multi-area power system: an adaptive fuzzy logic approach. IEEE Trans Power Syst 29(29):1822–1830
5. Ning C (2016) Robust H load-frequency control in interconnected power systems. IET Control Theory Appl 10(1):67–75
6. Han J (1998) Auto-disturbances-rejection controller and its applications. Control Decis 13 (1):19–23
7. Han J (2009) From PID to active disturbance rejection control. IEEE Trans Ind Electron 56 (3):900–906
8. Gao Z (2003) Scaling and parameterization based controller tuning. Proc Am Control Conf 6:4989–4996
9. Xue W, Huang C, Huang Y (2013) Design methods for the integrated guidance and control system. Control Theory Appl 30(12):1511–1520
10. Wang L, Tong C, Li Q, Yin Y, Gao Z, Zheng Q (2012) A practical decoupling control solution for hot strip width and gauge regulation based on active disturbance rejection. Control Theory Appl 29(11):1471–1478
11. Tan W (2010) Unified tuning of PID load frequency controller for power systems via IMC. IEEE Trans Power Syst 25(1):341–350
12. Hang C, Zheng Q (2014) Application of linear active disturbance rejection control to power system load frequency control. Int J Intell Control Syst 19(1):1–7
13. Pan W (2012) A new fruit fly optimization algorithm: taking the financial distress model as an example. Knowl Based Syst 26:69–74
14. Ning J, Wang B, Li H, Baohua X (2014) Research on and application of diminishing step fruit fly optimization algorithm. J Shenzhen Univ Sci Eng 31(4):367–373
15. Hang C, Gao Z (2013) On transfer function representation and frequency response of linear active disturbance rejection control. In: Proceedings of Chinese control conference, pp 72–77

Local Zernike Moment and Multiscale Patch-Based LPQ for Face Recognition

Xiaoyu Sun, Xiaoyan Fu, Zhuhong Shao, Yuanyuan Shang and Hui Ding

Abstract In this paper, a novel feature extraction method combining Zernike moment with multiscale patch-based local phase quantization is introduced, which can deal with the problem of uncontrolled image conditions in face recognition, such as expressions, blur, occlusion, and illumination changes (EBOI). First, the Zernike moments are computed around each pixel other than the whole image and then double moment images are, respectively, constructed from the real and imaginary parts. Subsequently, multiscale patch-based local phase quantization descriptor is utilized for the non-overlapping patches of moment images to obtain the texture information. Afterward, the support vector machine (SVM) is employed for classification. Experimental results performed on ORL, JAFFE, and AR databases clearly show that the LZM-MPLPQ method outperforms the state-of-the-art methods and achieves better robustness against severe conditions abovementioned.

Keywords Local Zernike moment · Local phase quantization · Face recognition · EBOI

1 Introduction

With the wide applications of surveillance, automation, and intelligent devices, face recognition (FR) has become one of the most active research areas of computer vision. Even though there are many methods proposed in FR [1–3] during the last

X. Sun · X. Fu (✉) · Z. Shao · Y. Shang · H. Ding
College of Information and Engineering, Capital Normal University, Beijing 100048, China
e-mail: fuxiaosg@163.com

X. Fu · Z. Shao · Y. Shang · H. Ding
Beijing Advanced Innovation Center for Imaging Technology, Capital Normal University, Beijing 100048, China

Y. Shang · H. Ding
Beijing Key Laboratory of Electronic System Reliability Technology, Capital Normal University, Beijing 100048, China

© Springer Science+Business Media Singapore 2016

Y. Jia et al. (eds.), *Proceedings of 2016 Chinese Intelligent Systems Conference*, Lecture Notes in Electrical Engineering 405,
DOI 10.1007/978-981-10-2335-4_3

two decades, it is still a challenging problem to adapt different conditions such as expressions, blur, occlusion, and illumination changes (EBOI).

Generally, a FR system is constituted of feature extraction and pattern classification. It is of great significance to choose proper method to extract features. Global and local features are two classes of feature extraction methodologies. Since local features exemplified by LBP [4] and Gabor [5] have better affine invariance and illumination insensitivity compared with global features, they are usually applied to the FR system with changeable image variations. However, LBP gets poor antinoise ability while Gabor method suffers from high computational cost because of processing 40 components (5 scales and 8 orientations) for every facial image. In recent years, many other local feature methods have been proposed to achieve better performance. For example, Ojansivu and Heikkila [6] presented the local phase quantization method (LPQ) in discrete Fourier transform domain. To further improve the performance, LPQ family is enriched by patch-based LPQ [7] and adaptive LPQ [8]. Moreover, Chan [9] proposed an efficient method combining several multiscale feature descriptors, which achieved high classification rate and blur tolerance. On the other hand, the usages of Zernike moment (ZM) invariants [10, 11], which possess the properties of rotation invariance and less information redundancy, enabled to achieve successful recognition against expression variations [12] and occlusions [13]. However, ZM-based methods are usually used as global features, which negatively impact recognition rate in the images with illumination and blur.

In this work, a novel local face feature extraction method with the hybridization of local Zernike moment and multiscale patch-based LPQ is proposed, which is termed as LZM-MPLPQ and shows better robustness against the EBOI conditions. First, the Zernike moments are computed around each pixel to generate the moment images, which can better deal with expression changes and occlusion. Then, calculating by varying the filter size and combined histograms of all the LPQ regions obtained by dividing moment image into non-overlapping patches, we have the multiscale patch-based LPQ descriptor. MPLPQ is used to get stronger robustness to blur and illumination variations. In the proposed method, it is worth emphasizing that the real and imaginary components of ZM, which are extracted to avoid phase information redundancy considering the MPLPQ, are available to gain contour and shading information similar to the magnitude and phase components.

The proposed method is introduced in Sect. 2. Experimental results performed on several datasets are provided in Sect. 3, and Sect. 4 concludes the paper.

2 The Proposed Method

To develop a novel face extraction method that is insensitive to EBOI, we propose to use a combination with two descriptors: local Zernike moment and local phase quantization. And we investigate how they are useful for face recognition invariant to environment conditions. In the following, we introduce these methods in detail.